AGU PUBLICATIONS

JGR

Journal of Geophysical Research: Biogeosciences

RESEARCH ARTICLE
10.1002/2015JG003149

Key Points:
- Leaf litter is a significant COS sink in a mediterranean oak woodland
- Drying-rewetting cycles produce bursts in litter COS and CO_2 fluxes
- Litter COS uptake reduces the amount of COS available for soil uptake

Supporting Information:
- Supporting Information S1

Correspondence to:
W. Sun and U. Seibt,
wu.sun@ucla.edu;
useibt@ucla.edu

Citation:
Sun, W., K. Maseyk, C. Lett, and U. Seibt (2016), Litter dominates surface fluxes of carbonyl sulfide in a Californian oak woodland, *J. Geophys. Res. Biogeosci.*, *121*, 438–450, doi:10.1002/2015JG003149.

Received 11 JUL 2015
Accepted 21 JAN 2016
Accepted article online 25 JAN 2016
Published online 13 FEB 2016

Litter dominates surface fluxes of carbonyl sulfide in a Californian oak woodland

Wu Sun[1], Kadmiel Maseyk[2,3], Céline Lett[2,4], and Ulli Seibt[1,2]

[1]Department of Atmospheric and Oceanic Sciences, University of California, Los Angeles, California, USA, [2]Institute of Ecology and Environmental Sciences, Université Pierre et Marie Curie, Paris, France, [3]Now at Department of Environment, Earth and Ecosystems, Faculty of Science, Open University, Milton Keynes, UK, [4]Now at British Antarctic Survey, Cambridge, UK

Abstract Carbonyl sulfide (COS) is a promising tracer for partitioning terrestrial photosynthesis and respiration from net carbon fluxes, based on its daytime co-uptake alongside CO_2 through leaf stomata. Because ecosystem COS fluxes are the sum of plant and soil fluxes, using COS as a photosynthesis tracer requires accurate knowledge of soil COS fluxes. At an oak woodland in Southern California, we monitored below-canopy surface (soil + litter) COS and CO_2 fluxes for 40 days using chambers and laser spectroscopy. We also measured litter fluxes separately and used a depth-resolved diffusion-reaction model to quantify the role of litter uptake in surface COS fluxes. Soil and litter were primarily COS sinks, and mean surface COS uptake was small (~1 pmol m^{-2} s^{-1}). After rainfall, uptake rates were higher (6–8 pmol m^{-2} s^{-1}), and litter contributed a significant fraction (up to 90%) to surface fluxes. We observed rapid concurrent increases in COS uptake and CO_2 efflux following the onset of rain. The patterns were similar to the Birch effect widely documented for soils; however, both COS and CO_2 flux increases originated mainly in the litter. The synchronous COS-CO_2 litter Birch effect indicates that it results from a rapid increase in litter microbial activity after rainfall. We expect that the drying-rewetting cycles typical for mediterranean and other semiarid ecosystems create a pronounced seasonality in surface COS fluxes. Our results highlight that litter uptake is an important component of surface COS exchange that needs to be taken into account in ecosystem COS budgets and model simulations.

1. Introduction

Carbonyl sulfide (COS), a trace gas in the atmosphere (~484 pmol mol^{-1}), has been recently recognized as a promising indicator of gross photosynthetic carbon flux in terrestrial ecosystems due to its close coupling with CO_2 during leaf uptake [*Montzka et al.*, 2007; *Campbell et al.*, 2008; *Asaf et al.*, 2013; *Berry et al.*, 2013]. This coupling is a result of codiffusion of CO_2 and COS into leaf stomata [*Sandoval-Soto et al.*, 2005; *Seibt et al.*, 2010; *Stimler et al.*, 2010], and subsequent hydrolysis mediated by carbonic anhydrase (CA) enzymes [*Protoschill-Krebs and Kesselmeier*, 1992; *Protoschill-Krebs et al.*, 1996; *Schenk et al.*, 2004; *Notni et al.*, 2007]: $COS + H_2O \rightarrow H_2S + CO_2$. This hydrolytic reaction can also happen in soils, complicating the link between ecosystem COS and CO_2 uptake.

The global biogeochemical cycle of COS is predominantly driven by vegetation and soil microbial uptake, and production from ocean biogenic activities and photochemical reactions [*Kettle et al.*, 2002; *Berry et al.*, 2013]. Other known significant COS sources include anthropogenic emissions [*Campbell et al.*, 2015] and biomass burning [*Campbell et al.*, 2015; *Blake et al.*, 2004; *Montzka et al.*, 2007], both of which are much smaller than the vegetation sink. The seasonal amplitudes of atmospheric COS and CO_2 concentrations in the Northern Hemisphere are highly correlated [*Montzka et al.*, 2007]. Regional atmospheric drawdown and ecosystem and leaf level fluxes of COS and CO_2 also exhibit strong covariation [*Campbell et al.*, 2008; *Asaf et al.*, 2013; *Stimler et al.*, 2010]. The COS tracer approach to gross primary productivity is promising because COS plant uptake appears to dominate the continental COS budget. However, other continental sources and sinks, in particular those in soils, need to be better understood to develop a robust tracer approach.

The catalytic reaction between COS and CA enzymes in soils is indicated by the reduced COS uptake after treatment with CA inhibitor [*Kesselmeier et al.*, 1999], and by the oxygen isotope signatures of soil CO_2 efflux [*Seibt et al.*, 2006; *Wingate et al.*, 2009]. Soil COS uptake is a function of temperature, soil porosity, and water content, with different optimum temperatures and water contents identified for a range of soils in laboratory

experiments [*Kesselmeier et al.*, 1999; *Van Diest and Kesselmeier*, 2008; *Whelan et al.*, 2015]. In field studies, soil COS uptake has been observed in a handful of ecosystems. Soil uptake rates of COS measured in the field are mostly in the order of 1–10 pmol m^{-2} s^{-1} [*Castro and Galloway*, 1991; *Simmons et al.*, 1999; *Yi et al.*, 2007; *Berkelhammer et al.*, 2014; *Maseyk et al.*, 2014]. Larger soil uptake rates have been observed in an oak woodland in Northern California but were likely biased by pressure-driven advection [*Kuhn et al.*, 1999]. Leaf litter also acted as a COS sink [*Kesselmeier and Hubert*, 2002; *Berkelhammer et al.*, 2014], contributing a significant fraction of surface fluxes in a subtropical forest [*Yi et al.*, 2007]. Although the majority of observations have shown that soils generally behave as COS sinks, the presence of a compensation point [*Kesselmeier et al.*, 1999; *Conrad and Meuser*, 2000; *Liu et al.*, 2010] indicates that COS may also be produced in the soil. Net emissions of COS have been observed in a wheat field soil at high temperature [*Maseyk et al.*, 2014] and samples from a range of other oxic soils [*Whelan et al.*, 2015], and in anoxic soils such as those in peatlands, salt marshes, and flooded paddy fields [*de Mello and Hines*, 1994; *Li et al.*, 2006; *Yi et al.*, 2008, 2013; *Whelan et al.*, 2013].

However, most of the field studies were conducted using temporally sparse sampling, limiting our ability to link COS fluxes to environmental and biological factors. Therefore, soil COS fluxes have been either assumed to be negligible [*Asaf et al.*, 2013], or empirically parameterized from soil respiration and moisture [*Berry et al.*, 2013] or H_2 fluxes [*Launois et al.*, 2015]. Litter fluxes have rarely been quantified separately in the field [*Berkelhammer et al.*, 2014] and are not included yet in any budget or modeling studies.

Here we analyze the response of soil and litter COS fluxes to environmental conditions during a 40 day field campaign in an oak woodland in Southern California in spring 2013. We quantify the contributions of litter uptake to the net surface fluxes of both COS and CO_2 using a depth-resolved diffusion-reaction model that includes an interactive litter layer [*Sun et al.*, 2015]. Our study addresses a crucial gap in closing ecosystem COS budgets, an important step toward a COS-based carbon flux partitioning approach.

2. Methods and Materials

2.1. Field Site

We conducted measurements from 1 April to 11 May 2013 (day of year (DOY) 91–131) at the Stunt Ranch UC Reserve (34°05′38″ N, 118°39′26″ W, 397 m above sea level) in the Santa Monica Mountains, California. The study site was in a mediterranean oak woodland dominated by coast live oak (*Quercus agrifolia*). The soil is a gravelly loam [*USDA Soil Survey*, 2014], covered by a 2–6 cm thick layer of leaf litter. Annual rainfall was about 180 mm in 2012–2013, mostly received during the winter, and average annual temperature is 19°C (July: 24°C, January: 14°C). The site has large interannual variability in precipitation. Rainfall was observed on 31 March (DOY 90, 2 mm) and 5–6 May (DOY 125–126, 13.5 mm, see Figure S1 in the supporting information (SI)).

2.2. Experimental Setup

A mid-infrared quantum cascade laser (QCL) spectrometer (Aerodyne Research Inc., Billerica, MA) was used to measure COS, CO_2, and H_2O concentrations. The RMS noise (1σ) at 1 Hz was 3–5 parts per trillion by volume for COS. Flow through the instrument was maintained by a TriScroll 600 pump (Agilent Technologies) connected to the analyzer by a 1 inch vacuum line. The analyzer was housed in a small shed that was ventilated but not temperature controlled. To account for instrument drift due to temperature changes, we implemented frequent background calibrations (every 15 min) with dry N_2 as the zero gas and corrected the drift linearly in all calculations (Text S2 in the SI). A solenoid valve at the analyzer inlet was actuated to switch from the sampling line to the background/zero gas. Due to insufficient background correction, the measured gas concentrations were affected by instrument drift on 1–2 April (DOY 91–92). The calculated chamber fluxes were not affected because they are based on relative concentration changes.

We deployed two chambers for soil flux observations. The chambers were modified versions of LI-8100 long-term soil chambers (LI-COR Biosciences Inc., Lincoln, NE), with custom-made stainless steel chamber bowls and collars. A third, identical chamber was used as a blank control chamber by sealing the bottom with Teflon FEP film (see SI for details on uncertainty estimates). Soil chamber 1 (SC1) was placed 4.5 m away from a coast live oak tree, SC2 was 0.5 m away from the tree, and underneath the tree canopy. The litter layer was 2 cm thick in SC1, and 6 cm thick in SC2. We kept the litter in the chambers intact as much as possible. The soil chambers were connected to the COS analyzer via 1/4 inch sampling lines (Synflex tubing). Teflon filters (1 μm Millipore Millex) were placed at each chamber sampling line and at the analyzer inlet to prevent particle contamination. To keep all sampling lines flushed at all times, a second dry scroll pump (IDP3, Agilent) was used to provide bypass flow for the lines not directed into the QCL. The bypass flow was directed via 1/4 inch

Dekabon tubing back into the chambers to provide the incoming air for the chamber measurements. The flow rate of the incoming air was adjusted with needle valves to provide slightly more flow (0.1 to 0.2 standard liter per minute) into the chamber than pulled through the outlet. The open vent on top of the chamber provided sufficient release for the small additional incoming flow to maintain ambient pressure inside the chamber.

Flow rates in the sampling lines were monitored with flowmeters (Honeywell AWM5104VN). We also measured atmospheric temperature and humidity (Vaisala HMP 45 AC probes), chamber air temperatures (type T thermocouples, PFA coated), and soil temperatures and volumetric soil water content (SWC) in the upper 5 cm (Stevens Hydra Probe II, Stevens Water Monitoring Systems Inc., Portland, OR). A data logger (CR1000, Campbell Scientific Inc., Logan, UT) was used to control the opening and closing of chambers, and switching of solenoid valves to select sampling lines, and record sensor data. Chambers were sampled in 15 min intervals, with zero offset correction at the start of each interval. Chambers were closed for 8 min, with the transient changes in chamber air concentrations monitored by the QCL. Before and after chamber closure, the air in the open chamber was measured for 2 min each. Chamber fluxes were calculated from the differences between the transient changes and the incoming air concentrations interpolated from the two open chamber measurements (see Figure S2 in the SI). Each soil chamber was sampled once per 90 min period (before DOY 116) or per 120 min period (after DOY 116).

2.3. Litter Incubation Experiments

To constrain the litter fluxes, we conducted two litter incubation experiments from 7 to 9 and 9 to 11 May (DOY 127–129, 129–131). Litter samples were collected from the area between the two soil chambers and from a similar footprint to the chambers, placed in SC3, and measured as part of the sampling sequence. The samples as well as in situ litter content of the soil chambers were then collected for laboratory analysis of litter wet and dry weights (Table S1 in the SI).

Litter fluxes of COS (F_{SL}, pmol kg^{-1} s^{-1}) and CO_2 (F_{CL}, μmol kg^{-1} s^{-1}, both per unit litter dry weight) were assumed to be functions of litter temperature (T_L, K, approximated by the air temperature in the incubation chamber) and litter water content (w_L, g water g^{-1} litter). Changes in water content of the litter samples were calculated by integrating litter water fluxes over time. We formulated nonlinear regression models for litter COS and CO_2 fluxes (see Text S3 in the SI):

$$F_{SL}(w_L, T_L, C_{S,a}) = V_{SLU,max} \cdot \sinh(k_{SL} w_L) \cdot k_{H,S}(T_L) \cdot C_{S,a} + V_{SLP,max} \cdot \exp[k_T(T_L - T_{ref})] \quad (1)$$

$$F_{CL}(w_L, T_L) = V_{CLP,max} \cdot \sinh(k_{CL} w_L) \cdot \exp\left[-\frac{E_{RL}}{R}\left(\frac{1}{T_L} - \frac{1}{T_{ref}}\right)\right] \quad (2)$$

where $V_{SLU,max}$ (m^3 kg^{-1} s^{-1}) and $V_{SLP,max}$ (pmol kg^{-1} s^{-1}) are the baseline rates of litter COS uptake and production (i.e., uptake/production capacity), $V_{CLP,max}$ (μmol kg^{-1} s^{-1}) is the baseline rate of litter respiration (i.e., CO_2 production capacity), k_T (K^{-1}) is the temperature dependence factor for COS production which is equivalent to $Q_{10} = 1.9$ (see Text S3 in the SI), $T_{ref} = 25$°C is a reference temperature, k_{SL} and k_{CL} (both dimensionless) are moisture limitation factors for COS uptake and CO_2 production, E_{RL} (J mol^{-1}) is the activation energy of litter respiration, and $k_{H,S}$ (dimensionless) is the Henry's law constant for COS. We obtained a new equation for $k_{H,S}(T)$ from a fit to empirical data [*Elliott et al.*, 1989]:

$$k_{H,S}(T) = (T/\mathrm{K}) \exp\left(\alpha + \frac{\beta}{T/\mathrm{K}}\right) \quad (3)$$

with parameters $\alpha = -20.00$ and $\beta = 4050$ [*Sun et al.*, 2015]. The term $k_{H,S}(T)$ is applied to the ambient concentration, $C_{S,a}$ (pmol m^{-3}), to get the aqueous concentration of COS, since COS hydrolysis typically occurs in the aqueous phase. Hyperbolic functions are chosen for moisture dependence so that fluxes approach zero in completely dry conditions. Outliers were excluded from the regression of litter fluxes by using Cook's distance statistic [*Cook*, 1977]. The fit parameters from equations (1) and (2) were then used to parameterize litter fluxes in the soil-litter flux model described below.

2.4. Litter and Soil Environmental Variables

Litter porosity was estimated to be 0.94 (Text S4 in the SI). The litter water content was calculated by integrating litter water fluxes from multiple regressions of litter incubation data (Figures S6 and S7 in the SI).

Due to the lack of direct field data, the initial litter moisture and that after the second rain (DOY 126) were set to about half of the observed litter water content at saturation (Table S5) to fit the observed COS fluxes and the litter water content measured prior to the litter incubations.

Soil porosity was measured as 0.35 m^3 m^{-3}. At the soil-litter interface, porosity values were interpolated to prevent numerical instability caused by discontinuity. Soil temperature and moisture profiles were parameterized from the values measured at 5 cm depth. We assume that the temperature variations are a superposition of fast varying diurnal sine waves and slowly varying background signals [*Van Wijk and de Vries*, 1963]. Temperatures of deeper soil that are not measured are constructed by superposing the background signals with depth-damped, phase-lagged diurnal variations (Text S5 and Figure S9 in the SI). We assumed that soil water content is 0.20 m^3 m^{-3} at 1 m depth, corresponding to typical field capacity of loamy soils [*Or and Wraith*, 2002]. Soil water content profiles were constructed from data collected at 5 cm depth assuming a smooth increase with depth (Figure S8 and Table S6 in the SI).

2.5. Modeling Surface (Soil + Litter) Fluxes

We use a depth-resolved diffusion-reaction model to simulate surface COS and CO_2 fluxes from soil parameters and environmental variables, with flux activity in the litter included. A detailed description as well as evaluation of the COS model is presented in *Sun et al.* [2015]. Briefly, the model evaluates COS profiles accounting for vertical diffusion and local sources and sinks. The source and sink terms are related to temperature and moisture in each soil/litter layer. Here we incorporate a CO_2 model with the same structure as the COS model but its own production terms.

Briefly, the soil COS sink term is parameterized as the soil COS uptake capacity ($V_{SSU,max}$, mol m^{-3} s^{-1}) multiplied by temperature and moisture limitation functions [*Sun et al.*, 2015]. The soil COS production term is the COS production capacity ($V_{SSP,max}$, mol m^{-3} s^{-1}) modified by an exponential temperature function with $Q_{10} = 1.9$ [*Sun et al.*, 2015; *Maseyk et al.*, 2014].

For CO_2 fluxes, the soil CO_2 source term is

$$P_C(T, w_S, z) = V_{CSP,max} \cdot f_C(T) \cdot w_S/w_0 \cdot \exp(-z/z_D) \quad (4)$$

where $V_{CSP,max}$ (mol m^{-3} s^{-1}) is the CO_2 production capacity, $f_C(T)$ is the temperature limitation function, w_S/w_0 is the linear moisture dependence function with $w_0 = 0.10$, and $z_D = 0.2$ m is assumed for the exponential decay depth for the CO_2 production profile. The temperature dependence $f_C(T)$ was adapted from the widely used modified Arrhenius equation [*Lloyd and Taylor*, 1994] but was normalized so that $f_C(T_{ref} = 25°C) = 1$. The V_{max} parameters ($V_{SSU,max}$, $V_{SSP,max}$, and $V_{CSP,max}$) are optimized by minimizing the sum of square errors cost function (model result versus observations) with the gradient descent or Newton's method.

Litter source and sink terms of COS and CO_2 are described in equations (1) and (2). For model implementation, the litter COS uptake and production capacities ($V_{SLU,max}$ and $V_{SLP,max}$) and CO_2 production capacity ($V_{CLP,max}$) were converted from per unit litter dry weight to per unit volume of litter (mol m^{-3} s^{-1}) using the litter dry bulk density (31.3 kg m^{-3}, see Text S4 in the SI).

3. Results

3.1. Surface (Soil + Litter) Fluxes

During the campaign, both observed surface areas behaved primarily as net COS sinks, with fluxes from −6.3 to +3.0 and from −7.9 to +2.5 pmol m^{-2} s^{-1} in chambers 1 and 2, respectively, and an overall mean flux of −1 pmol m^{-2} s^{-1} (Table 1 and Figure 1a). Net emissions were observed in 15% of measurements, mostly associated with soil temperatures above 15°C (Figure S11a in the SI). Larger emissions (> +1 pmol m^{-2} s^{-1}) were only observed in 1% of cases.

The overall trends of surface COS fluxes in the two chambers were very similar and generally followed changes in soil moisture (Figure 1). COS uptake was strongest after rain events, peaking at −6 to −8 pmol m^{-2} s^{-1} and gradually decreasing to about −1 pmol m^{-2} s^{-1} within 10 days after the rain. The peak COS fluxes in both chambers lagged the rain event on DOY 126 by approximately 1 day. The diurnal variations of COS fluxes resembled those in soil temperature (Figure 2c) and were small compared to the long-term variations. Diurnal amplitudes of COS fluxes were smallest during the dry period. CO_2 fluxes showed broadly similar temporal patterns as COS fluxes (Figure 1b). In contrast to the COS fluxes, however, the CO_2 fluxes were very different between the two chambers, probably due to root respiration as SC2 was located next to a tree.

Table 1. Summary of Observations and Model Results for Chamber Fluxes

	SC1	SC2
Maximum surface COS flux (pmol m^{-2} s^{-1})	2.95	2.47
Minimum surface COS flux (pmol m^{-2} s^{-1})	−6.33	−7.85
Mean surface COS flux (pmol m^{-2} s^{-1})	−1.13	−1.43
Mean surface CO_2 flux, observed (μmol m^{-2} s^{-1})	0.54	1.19
Mean soil water content (m^3 m^{-3})	0.138	0.035
Litter thickness (cm)	2	6
Mean modeled surface COS flux (pmol m^{-2} s^{-1})	−1.02	−1.28
Mean modeled surface CO_2 flux (μmol m^{-2} s^{-1})	0.63	1.13
RMSE of modeled COS fluxes (pmol m^{-2} s^{-1})	0.85	0.83
RMSE of modeled CO_2 fluxes (μmol m^{-2} s^{-1})	0.49	0.63
Pearson correlation, model versus observation COS fluxes	0.801	0.884
Pearson correlation, model versus observation CO_2 fluxes	0.436	0.717
Range of modeled litter COS fluxes (pmol m^{-2} s^{-1})	−5.95 to +0.25	−6.85 to +0.74
Mean modeled litter COS flux (pmol m^{-2} s^{-1})	−0.58	−1.10
Mean litter contribution to COS soil + litter uptake	56.9%	85.7%
Mean litter contribution to COS soil + litter uptake, first five days (after rain)	83.5%	95.6%
Mean modeled litter CO_2 flux (μmol m^{-2} s^{-1})	0.21	0.51
Mean litter contribution to CO_2 emissions	34.2%	44.8%
Mean litter contribution to CO_2 emissions, first five days (after rain)	71.7%	74.2%

For both chambers, net COS uptake increased exponentially with soil water content (SWC), with a similar shape of the SWC response (Figure 2a). Surprisingly, the two curves appear shifted along the SWC axis, indicating that changes in the surface COS flux are related to soil moisture variations but soil moisture is not the main driver of the COS fluxes at our site (see section 4). Net COS and CO_2 fluxes were negatively correlated in both chambers (Figure 2b), consistent with previous observations [*Yi et al.*, 2007; *Berkelhammer et al.*, 2014].

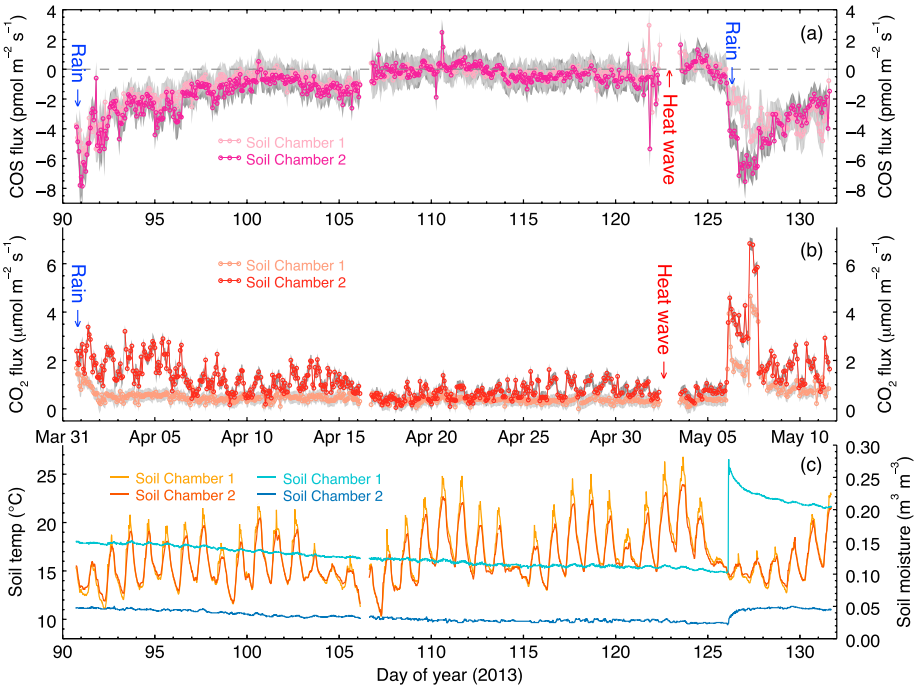

Figure 1. Observed surface fluxes of (a) COS and (b) CO_2 measured in two soil chambers at an oak woodland in Southern California in spring 2013 (1 April to 11 May, DOY 91–131), with (c) soil temperatures and volumetric soil water content. Shaded areas are 95% confidence intervals of fluxes, including uncertainty estimates from blank chamber measurements (see SI). Arrows indicate two rain events and a heat wave. Note that SC1 had much less litter and was farther from the tree than SC2.

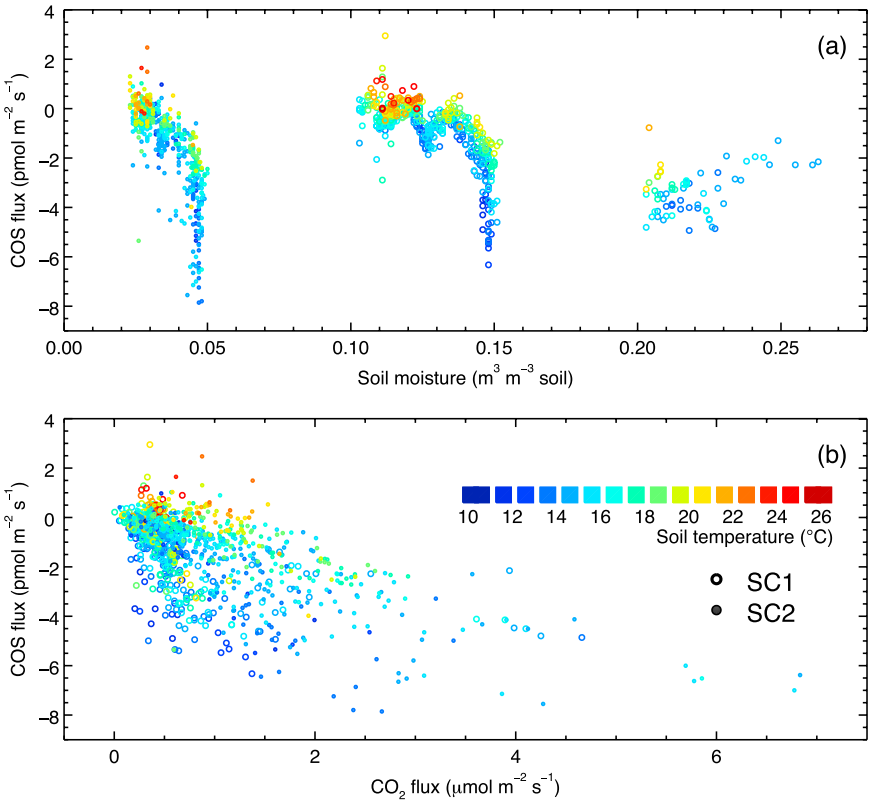

Figure 2. The observed surface COS fluxes appear to have different relationships with (a) soil water content for the two soil chambers, although the overall shape of the SWC response is similar for both chambers. (b) Surface COS uptake is positively correlated with CO_2 efflux in both chambers. Data points are colored for soil temperatures.

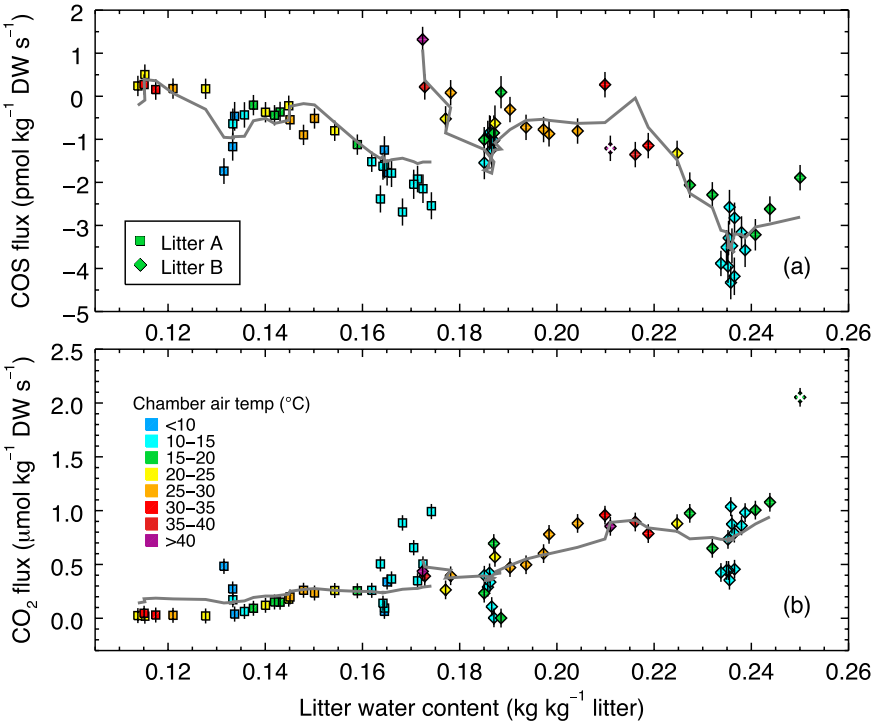

Figure 3. Litter (a) COS and (b) CO_2 fluxes observed in two incubation experiments using litter collected at the site. Error bars show $\pm 1\sigma$ ranges with blank chamber effect included. Colors of data points indicate temperature bins. Also shown are fitted litter fluxes (grey, equations (1) and (2)). Outliers (marked by white crosses) were excluded from the regressions.

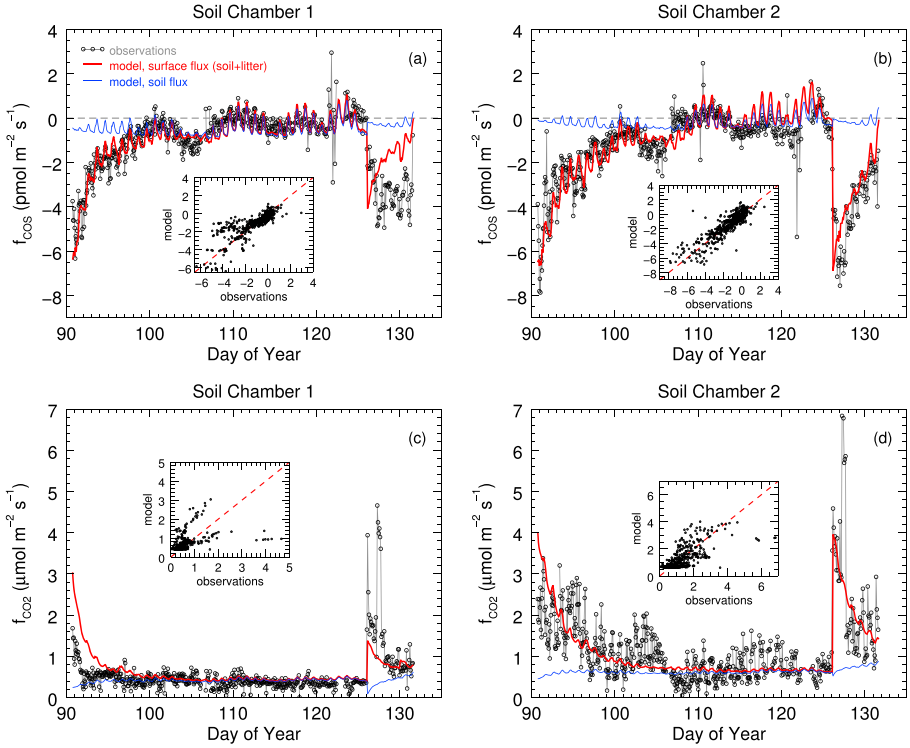

Figure 4. Modeled surface (soil + litter) (a, b) COS and (c, d) CO_2 fluxes (red) in the two soil chambers agree well with observations (black) during most of the campaign (panel insets show modeled versus observed fluxes). Also shown are the fluxes simulated at the litter-soil interface, i.e., resulting from soil-only gas exchange (blue).

3.2. Litter Fluxes

In both incubation experiments, the leaf litter of coast live oak was mostly a net COS sink, with fluxes ranging from −4.3 to +1.3 pmol s^{-1} kg^{-1} dry weight (Figure 3a), and a source of CO_2 (Figure 3b). Litter COS uptake and CO_2 production decreased as the litter was drying over time (fluxes in Figure 3 are plotted versus litter moisture). Based on nonlinear fits (equations (1) and (2)), we found a strong relationship between COS and CO_2 fluxes and litter moisture, but only a weak correlation with temperature. Deviations from the fit were observed below 15°C at night (Figure 3) and associated with high relative humidity, probably due to dew formation on the litter surface. Dew formation would result in increased litter moisture not detected by our water flux measurements. COS uptake and CO_2 production were well correlated (Figure S4 in the SI), with stronger correlation when chamber air temperature was below 15°C ($r = -0.77$). At higher temperature, the correlation between the fluxes was weaker ($r = -0.65$) as litter CO_2 fluxes had a stronger temperature response than COS fluxes.

4. Discussion

4.1. Litter is a Major Contributor to Surface COS Fluxes

Using the depth-resolved model to quantify the contributions from litter and soil to net surface fluxes (Figure 4), we found that litter uptake accounted for the majority of COS fluxes during wet periods, and nearly the entire flux for SC2 (Table 1 and Figure 5). During the dry period, litter still contributed substantially to fluxes in SC2 but very little in SC1. The net surface COS fluxes should therefore be plotted against the litter moisture as the relevant parameter in Figure 2a. Since we did not record continuous litter moisture data, the fluxes are plotted against soil moisture that has similar changes over time, but the plots appear shifted since the soil moisture was significantly lower in SC2 throughout the campaign.

Several factors may explain the stronger role of litter fluxes in SC2. Since SC2 was located directly under the large tree, it had a much thicker litter layer than SC1 (6 cm versus 2 cm) and hence more litter COS uptake. The litter in SC2 should also have a lower rate of water loss because of the insulating effect of the thicker layer, and due to the lower temperatures (Figure 1c) in its shaded location next to a tree. The resulting higher litter moisture in SC2 during the dry period is represented in the model (Figure S7 in the SI). The stronger

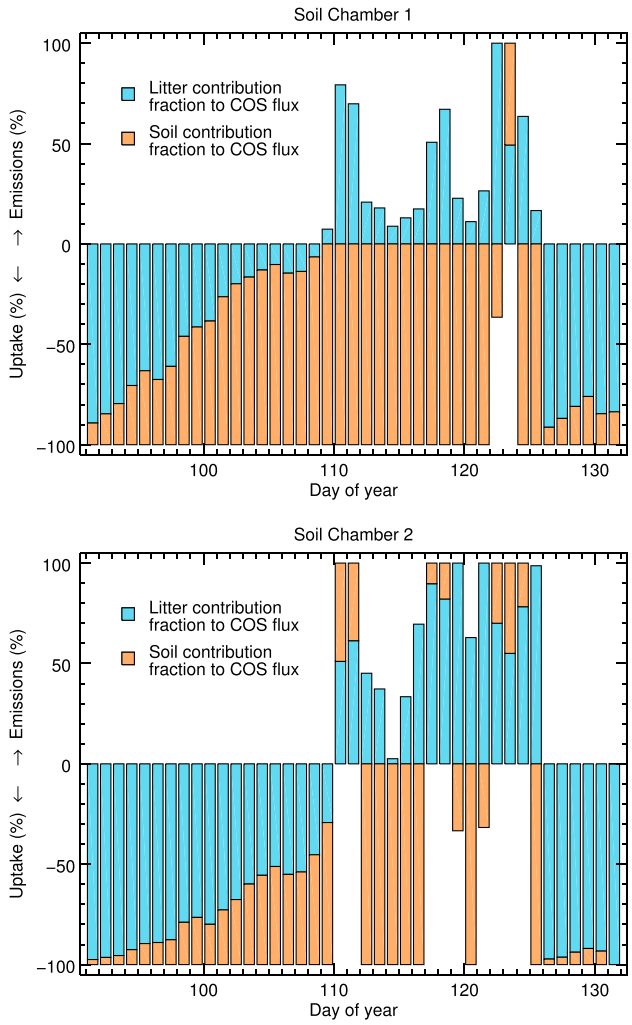

Figure 5. Relative contributions of litter and soil components to daily mean chamber COS fluxes from model results. Note that emissions were much smaller than uptake fluxes (see Figure 4). Litter and soil fluxes with different signs were normalized against the larger component (e.g., between DOY 110 and 125).

COS uptake in the thicker and more humid litter in SC2 then leads to a stronger COS drawdown across the litter layer so that less COS reaches the soil (Figure S12 in the SI). In addition, SC2 had lower soil moisture due to water uptake by the roots of the nearby tree. The soil under SC2 should therefore have lower microbial activity due to the lower moisture and additionally lower microbial COS uptake due to the lower soil COS concentration. However, the stronger litter COS uptake more than compensates for the lower soil uptake in SC2, particularly during wet periods. In oak woodlands and other ecosystems with a sparse or open canopy, we thus expect overall stronger, and more litter-dominated, surface COS fluxes near and under the trees than in the intercanopy space. As discussed below, we also expect litter COS uptake to play a major role in surface COS fluxes and thus surface COS fluxes to reflect the distribution and timing of litter fall and decomposition across many ecosystems.

The litter in our field incubations had fluxes ranging from −4.3 to +1.3 pmol s^{-1} kg^{-1} dry weight (section 3.2), comparable to litter fluxes of −2.7 to +1.6 pmol s^{-1} kg^{-1} dry weight from a beech forest measured in laboratory incubations [*Kesselmeier and Hubert*, 2002]. *Kesselmeier and Hubert* [2002] also observed increasing litter COS uptake with litter moisture up to approximately 25–45%, although the litter moisture in our field incubations (10–25%) was at the lower end of their range. For soil samples from our site, the largest observed COS uptake rate was about 0.3 pmol kg^{-1} s^{-1} from laboratory incubations, with a similar range as measured for samples from other natural ecosystems [*Whelan et al.*, 2015].

4.2. Litter Moisture Changes Drive Variations in Surface COS and CO_2 Fluxes

We observed strong concurrent increases in surface COS uptake and CO_2 emissions after rain (Figure 6). Combining the surface flux and litter incubation data with model simulations indicates that this increase predominantly originated from the litter layer (Figure 4), with more than 80% of COS uptake and more than 70% of CO_2 emissions attributed to the litter layer in the first five days after the rain event (Table 1). The response of both fluxes to rainfall is similar to the Birch effect—the burst of CO_2 efflux after rewetting of dry soils [*Birch*, 1958; *Jarvis et al.*, 2007]. However, at our site the flux spikes were dominated by litter fluxes, with only a minor contribution from soil fluxes. In addition to the model analysis, our attribution is supported by the fact that the COS and CO_2 fluxes responded simultaneously (Figure 6). Second, the flux responses in SC2 were much stronger for both COS and CO_2 even though there was very little change in soil moisture underneath the tree canopy and thick litter layer (Figure 1).

Bursts of CO_2 emissions from litter following rewetting have been reported from laboratory studies [e.g., *Clein and Schimel*, 1994], but their contributions to surface fluxes in natural ecosystems have not been identified

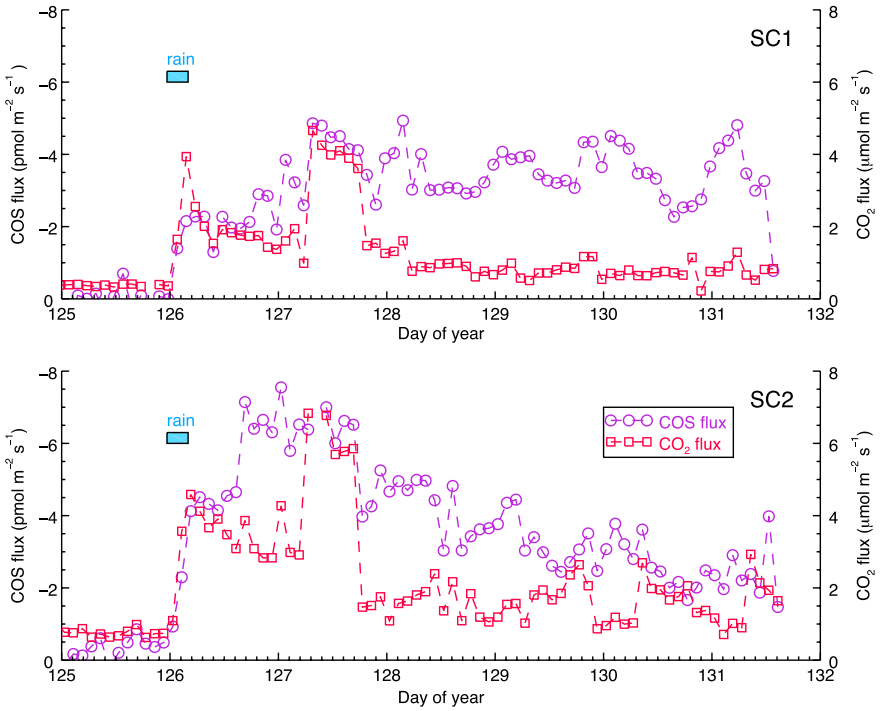

Figure 6. Rapid increases in COS and CO_2 fluxes immediately after the onset of rain on DOY 126 observed in both soil chambers. The peak fluxes occur with a lagged response, about one day after the rain. Note that the COS uptake is plotted on a reversed *y* axis.

yet. Based on our findings, we propose that leaf litter in the field can generate a Birch effect similar to that observed in soils. This litter Birch effect can occur even after light rainfall that is intercepted largely by the aboveground litter, with very little change in soil moisture. At the ecosystem scale, the rewetting of leaf litter may be an important contributor to the Birch effect observed in ecosystems with drying-rewetting cycles, for example, in mediterranean regions.

The physical destruction of soil aggregates should not play a role in the litter Birch effect, in contrast to the contribution of this process to the Birch effect in the soil [*Denef et al.*, 2001; *Navarro-García et al.*, 2012]. In the litter, labile carbon may have accumulated due to other mechanisms such as photodegradation [e.g., *Rutledge et al.*, 2010; *Wang et al.*, 2015] or the physical breaking up of leaves. The rapid mineralization of microbial compounds in response to rewetting identified in the soil [*Fierer and Schimel*, 2003] could also play a role in the litter. Further research is needed to identify which of these mechanisms may contribute to the litter Birch effect.

About one day after the rain, both COS and CO_2 fluxes show a second increase, with an earlier onset in the COS uptake than the CO_2 emissions (Figure 6). The difference in the timing of the second increase is likely due to the higher temperature sensitivity of litter respiration, whereas the enzyme activity responsible for COS uptake appears to be less sensitive to temperature. The time lag between first and second increases could indicate a sequential resuscitation of fast and slow responding microorganisms as observed in other ecosystems in California [*Placella et al.*, 2012], or a sequence of reactivation of microbes from dormancy followed by new microbial growth [*Fierer and Schimel*, 2003; *Blazewicz et al.*, 2014]. Microbial dynamics will need to be included explicitly to improve our capacity to simulate COS fluxes in environments with drying-rewetting cycles.

For the litter water content immediately after the rain (not measured), we used a best estimate of 0.3 g g^{-1} litter dry weight. This value fits well with the observed litter water content a few days after the rain (Figure S7) and is about half of the measured saturated litter water content of 0.5 to 0.6 g g^{-1} (Table S5 in the SI). To assess the potential effects of uncertainties in litter moisture on the litter-soil partitioning of COS uptake, we used an idealized simulation with no litter flux and enhanced soil uptake. However, even increasing the V_{max} for soil COS uptake by an order of magnitude cannot account for the high uptake after the rain because COS uptake does not respond linearly to V_{max} but rather logarithmically as it is limited by diffusion

[*Sun et al.*, 2015]. Considering that litter uptake draws down the COS concentration at the litter-soil boundary, it is even less likely that soil contributes a significant portion to the COS uptake after the rain.

We also observed an increase in COS uptake in both chambers during DOY 103–105, coincident with decreased soil temperatures and high relative humidity (Figure 1a and Figure S13 in the SI). This increase was likely caused by the lower soil and litter temperatures that reduced COS production, and possible dew formation on the litter surface that stimulated litter COS uptake.

4.3. Implications of Litter Fluxes for Soil Chamber Measurements

Chamber measurements of surface fluxes have been made either with the litter layer intact [*Castro and Galloway*, 1991; *Kuhn et al.*, 1999; *Yi et al.*, 2007] or with the aboveground litter removed from treatment plots [*Yi et al.*, 2007]. Litter fluxes have been reported separately in only one study so far [*Berkelhammer et al.*, 2014]: litter fluxes (-2.04 ± 0.4 pmol m^{-2} s^{-1}) were nearly identical to litter + soil fluxes (-2.1 ± 0.2 pmol m^{-2} s^{-1}), although the bare soil fluxes were larger (-4.4 ± 0.6 pmol m^{-2} s^{-1}). Our model simulations provide some insights into the mechanisms that may be responsible for this pattern. The strong uptake of COS in the litter layer leads to a significantly lower COS concentration at the litter-soil interface than in the ambient air at the litter surface (see Figure S12 in the SI). As enzymatic uptake depends on the COS concentration, the removal of the litter layer results in a much larger soil uptake flux due to the increased COS concentration in the soil air. Measuring soil fluxes with the litter removed therefore yields information on the potential soil uptake rather than the actual soil fluxes. Hence, removing the litter layer may lead to biases in measured COS uptake and CO_2 emissions, particularly in ecosystems with drying-rewetting cycles. Only during dry periods with small or no litter COS uptake does the litter layer behave as a diffusion barrier without a large effect on soil fluxes themselves.

As demonstrated by the results reported here and in *Berkelhammer et al.* [2014], the COS uptake of a soil-litter system is typically not the sum of fluxes measured from bare soil and litter samples. We therefore suggest that future studies report three fluxes: the surface flux from the intact litter-soil system, the bare soil flux after removing the litter, and the litter flux isolated from the soil underneath. A depth-resolved diffusion-reaction model can then be used to assess the contributions of litter and soil fluxes to the net surface COS flux [*Sun et al.*, 2015; *Ogée et al.*, 2015].

4.4. Dynamics of Surface COS Exchange in an Oak Woodland

The surface COS flux is controlled by physical and biological properties of the soil and overlying litter layers. At the Stunt Ranch site, water content was the dominant factor controlling the long-term trend of surface COS fluxes, whereas diurnal variations were mostly driven by temperature. We hypothesize that surface COS fluxes in ecosystems with seasonal rainfall such as mediterranean or other semiarid regions will have pronounced seasonal variations, with peaks in COS uptake following rain, and weak COS uptake or emissions during the dry season. Strong variations in the isotopic composition of soil CO_2 fluxes have also been reported in semiarid ecosystems [e.g., *Wingate et al.*, 2008; *Maseyk et al.*, 2009], indicating moisture-driven variations in microbial respiration and CA enzyme activity.

Litter phenology is likely another key factor controlling the seasonality of surface COS fluxes. In mediterranean ecosystems, many drought-deciduous species shed their leaves in the hot, dry summer period. Microbial activity is severely water limited during those months, and photochemical degradation plays a major role in litter decomposition [e.g., *Austin and Vivanco*, 2006]. The air-dried leaf litter accumulated on the ground provides structure and material (dormant microbial biomass or labile carbon) for the rapid onset of microbial activity after rainfall, i.e., the litter Birch effect associated with spikes in litter COS uptake. In contrast, in temperate ecosystems litter fall typically occurs in the autumn, and we would expect enhanced surface COS uptake around that time. However, litter decomposition then proceeds more gradually as long as there is sufficient soil moisture; hence, litter COS fluxes should be less variable than in semiarid systems. We therefore expect distinct patterns in the seasonality of surface COS fluxes for semiarid compared to other ecosystems.

4.5. Implications for COS-Enabled Land Biosphere Models

Incorporating COS as tracer into biosphere models has the potential to separate the responses of photosynthesis and respiration at large scales. However, few land surface models represent the litter as a separate layer even though a significant portion of land area is covered by aboveground litter [*Matthews*, 1997]. The lack of a litter layer may bias the net surface COS uptake if soil fluxes are parameterized from chamber measurements where the litter has been removed. For example, surface fluxes would be overestimated by a factor of 2

if based on the soil flux data instead of the soil + litter data reported in *Berkelhammer et al.* [2014]. Hence, neglecting litter uptake may lead to a potentially large bias in estimates of global surface COS fluxes. This would result in an equally large bias in vegetation COS uptake derived from flux budgets and be propagated into the COS-derived gross photosynthetic carbon uptake [see *Whelan et al.*, 2015].

In addition, our findings indicate that surface COS and CO_2 fluxes could be decoupled due to the effects of litter COS uptake. In the first study using a COS-enabled global biosphere model [*Berry et al.*, 2013], soil COS uptake was parameterized using the empirical relationship between COS uptake and microbial respiration [*Yi et al.*, 2007] and soil moisture limitation to diffusion [*Van Diest and Kesselmeier*, 2008]. Litter fluxes or soil COS production were not included. We tested two empirical COS-CO_2 relationships [*Berry et al.*, 2013; *Berkelhammer et al.*, 2014] using data from SC1 and found that they did not capture well the fluxes in the wet period (Figure S14 in the SI). The decoupling results from that litter fluxes dominate the net surface COS exchange while both litter and soil contribute to CO_2 emissions. For example, soil CO_2 production could proceed with very little associated COS uptake when a large amount of COS has already been converted in the litter layer. COS emitted during photodegradation [*Whelan and Rhew*, 2015] and soil COS production [*Maseyk et al.*, 2014] may additionally decouple COS and CO_2 fluxes at high solar radiation or soil temperatures.

Similar to the empirical COS-CO_2 relationships, the relationship with H_2 deposition that has been used to parameterize soil COS fluxes [*Launois et al.*, 2015] is likely an indirect link. In the soil, H_2 is mostly consumed by microbial hydrogenases (e.g., in *Streptomycetes* spp. [see *Constant et al.*, 2010]), and sometimes by methanogens and sulfate reducers [*Conrad*, 1996]. These processes do not appear to be directly linked to CA enzyme activity. Instead, the observed similarities in large-scale COS and H_2 deposition [*Belviso et al.*, 2013] could result from variations in microbial activity that affect different enzymes and hence both fluxes.

Instead of empirical relationships, depth-resolved models that treat COS as independent tracer [*Sun et al.*, 2015; *Ogée et al.*, 2015] are better suited for global COS simulations. However, we currently lack data on many of the model parameters. In our study, we were able to fit a single set of optimized COS uptake and production parameters for both chambers (Table S7 in the SI), indicating that similar mechanisms determine the flux patterns despite the differences in litter thickness and soil moisture. The optimized fluxes agreed well with observations in both chambers, which is encouraging for the use of biome-specific sets of parameters in large-scale models. Both chambers also had a similar optimum temperature for COS uptake of around 13°C (Figure S10 in the SI), comparable to a temperate arable soil (15°C) but lower than boreal soils (25°C) in lab incubations [*Van Diest and Kesselmeier*, 2008]. Temperature optima could be affected by changes in microbial community as well as varying contributions from different COS-converting enzymes [*Smeulders et al.*, 2011; *Ogawa et al.*, 2013] that may be present in addition to CA. COS models would therefore strongly benefit from data on enzyme activity linked to microbial community dynamics across biomes and seasons.

5. Conclusions

Our results indicate that litter plays a major role in determining surface COS fluxes in a mediterranean oak woodland. Litter water content was the most important driving factor for litter uptake, and thus also for net surface COS fluxes. Following a rainfall event, we observed a litter Birch effect with peaks in both COS and CO_2 fluxes, implying a rapid reactivation of litter microbes after rainfall. Surface COS fluxes are likely to show a distinct and pronounced seasonality in semiarid ecosystems. Due to the uptake of COS in the litter layer, combined with the concentration-dependent nature of soil COS uptake, the COS uptake by the intact litter-soil system is not the sum of the separate litter and soil components. It is therefore important to keep the litter-soil structure intact when installing chambers for surface COS measurements. Similarly, it is important to account for the litter-soil structure as well as litter fluxes in model simulations. Characterizing net surface, litter and bare soil COS fluxes separately will provide valuable new data and insights for model development and help to improve ecosystem to global COS budgets.

Acknowledgments

This study was supported by European Research Council (ERC) Starting Grant 202835 to U.S. W.S. acknowledges support by the China Scholarship Council (CSC) and the UC Institute for the Study of Ecological and Evolutionary Climate Impacts (ISEECI) GSR fellowships. We thank Phil Rundel for help and support during our field campaign, Mary Whelan for data sharing and valuable discussions, and support at the Stunt Ranch Santa Monica Mountains UC Reserve. Data presented here can be found in the University of California Curation Center (UC3) Merritt data repository at http://n2t.net/ark:/c5146/r3pp45, with doi:10.15146/R3PP45.

References

Asaf, D., E. Rotenberg, F. Tatarinov, U. Dicken, S. A. Montzka, and D. Yakir (2013), Ecosystem photosynthesis inferred from measurements of carbonyl sulphide flux, *Nat. Geosci.*, *6*(3), 186–190, doi:10.1038/ngeo1730.

Austin, A. T., and L. Vivanco (2006), Plant litter decomposition in a semi-arid ecosystem controlled by photodegradation, *Nature*, *442*, 555–558, doi:10.1038/nature05038.

Belviso, S., M. Schmidt, C. Yver, M. Ramonet, V. Gros, and T. Launois (2013), Strong similarities between night-time deposition velocities of carbonyl sulphide and molecular hydrogen inferred from semi-continuous atmospheric observations in Gif-sur-Yvette, Paris region, *Tellus B*, *65*, 20719, doi:10.3402/tellusb.v65i0.20719.

Berkelhammer, M., D. Asaf, C. Still, S. Montzka, D. Noone, M. Gupta, R. Provencal, H. Chen, and D. Yakir (2014), Constraining surface carbon fluxes using in situ measurements of carbonyl sulfide and carbon dioxide, *Global Biogeochem. Cycles*, *28*, 161–179, doi:10.1002/2013GB004644.

Berry, J., et al. (2013), A coupled model of the global cycles of carbonyl sulfide and CO_2: A possible new window on the carbon cycle, *J. Geophys. Res. Biogeosci.*, *118*, 842–852, doi:10.1002/jgrg.20068.

Birch, H. F. (1958), The effect of soil drying on humus decomposition and nitrogen availability, *Plant Soil*, *10*(1), 9–31, doi:10.1007/BF01343734.

Blake, N. J., et al. (2004), Carbonyl sulfide and carbon disulfide: Large-scale distributions over the western Pacific and emissions from Asia during TRACE-P, *J. Geophys. Res.*, *109*, D15S05, doi:10.1029/2003JD004259.

Blazewicz, S. J., E. Schwartz, and M. K. Firestone (2014), Growth and death of bacteria and fungi underlie rainfall-induced carbon dioxide pulses from seasonally dried soil, *Ecology*, *95*(5), 1162–1172, doi:10.1890/13-1031.1.

Campbell, J. E., et al. (2008), Photosynthetic control of atmospheric carbonyl sulfide during the growing season, *Science*, *322*(5904), 1085–1088, doi:10.1126/science.1164015.

Campbell, J. E., M. E. Whelan, U. Seibt, S. J. Smith, J. A. Berry, and T. W. Hilton (2015), Atmospheric carbonyl sulfide sources from anthropogenic activity: Implications for carbon cycle constraints, *Geophys. Res. Lett.*, *42*, 3004–3010, doi:10.1002/2015GL063445.

Castro, M. S., and J. N. Galloway (1991), A comparison of sulfur-free and ambient air enclosure techniques for measuring the exchange of reduced sulfur gases between soils and the atmosphere, *J. Geophys. Res.*, *96*(D8), 15,427–15,437, doi:10.1029/91JD01399.

Clein, J. S., and J. P. Schimel (1994), Reduction in microbial activity in birch litter due to drying and rewetting events, *Soil Biol. Biochem.*, *26*(3), 403–406, doi:10.1016/0038-0717(94)90290-9.

Conrad, R. (1996), Soil microorganisms as controllers of atmospheric trace gases (H_2, CO, CH_4, OCS, N_2O, and NO), *Microbiol. Rev.*, *60*(4), 609–640.

Conrad, R., and K. Meuser (2000), Soils contain more than one activity consuming carbonyl sulfide, *Atmos. Environ.*, *34*(21), 3635–3639, doi:10.1016/S1352-2310(00)00136-9.

Constant, P., S. P. Chowdhury, J. Pratscher, and R. Conrad (2010), Streptomycetes contributing to atmospheric molecular hydrogen soil uptake are widespread and encode a putative high-affinity [NiFe]-hydrogenase, *Environ. Microbiol.*, *12*(3), 821–829, doi:10.1111/j.1462-2920.2009.02130.x.

Cook, R. D. (1977), Detection of influential observation in linear regression, *Technometrics*, *19*(1), 15–18.

de Mello, W. Z., and M. E. Hines (1994), Application of static and dynamic enclosures for determining dimethyl sulfide and carbonyl sulfide exchange in *Sphagnum* peatlands: Implications for the magnitude and direction of flux, *J. Geophys. Res.*, *99*(D7), 14,601–14,607, doi:10.1029/94JD01025.

Denef, K., J. Six, K. Paustian, and R. Merckx (2001), Importance of macroaggregate dynamics in controlling soil carbon stabilization: Short-term effects of physical disturbance induced by dry-wet cycles, *Soil Biol. Biochem.*, *33*(15), 2145–2153, doi:10.1016/S0038-0717(01)00153-5.

Elliott, S., E. Lu, and F. S. Rowland (1989), Rates and mechanisms for the hydrolysis of carbonyl sulfide in natural waters, *Environ. Sci. Technol.*, *23*(4), 458–461, doi:10.1021/es00181a011.

Fierer, N., and J. P. Schimel (2003), A proposed mechanism for the pulse in carbon dioxide production commonly observed following the rapid rewetting of a dry soil, *Soil Sci. Soc. Am. J.*, *67*(3), 798–805, doi:10.2136/sssaj2003.7980.

Jarvis, P., et al. (2007), Drying and wetting of Mediterranean soils stimulates decomposition and carbon dioxide emission: The "Birch effect", *Tree Physiol.*, *27*(7), 929–940, doi:10.1093/treephys/27.7.929.

Kesselmeier, J., and A. Hubert (2002), Exchange of reduced volatile sulfur compounds between leaf litter and the atmosphere, *Atmos. Environ.*, *36*(29), 4679–4686, doi:10.1016/S1352-2310(02)00413-2.

Kesselmeier, J., N. Teusch, and U. Kuhn (1999), Controlling variables for the uptake of atmospheric carbonyl sulfide by soil, *J. Geophys. Res.*, *104*(D9), 11,577–11,584, doi:10.1029/1999JD900090.

Kettle, A. J., U. Kuhn, M. von Hobe, J. Kesselmeier, and M. O. Andreae (2002), Global budget of atmospheric carbonyl sulfide: Temporal and spatial variations of the dominant sources and sinks, *J. Geophys. Res.*, *107*(D22), 4658, doi:10.1029/2002JD002187.

Kuhn, U., C. Ammann, A. Wolf, F. Meixner, M. Andreae, and J. Kesselmeier (1999), Carbonyl sulfide exchange on an ecosystem scale: Soil represents a dominant sink for atmospheric COS, *Atmos. Environ.*, *33*(6), 995–1008, doi:10.1016/S1352-2310(98)00211-8.

Launois, T., P. Peylin, S. Belviso, and B. Poulter (2015), A new model of the global biogeochemical cycle of carbonyl sulfide—Part 2: Use of carbonyl sulfide to constrain gross primary productivity in current vegetation models, *Atmos. Chem. Phys.*, *15*, 9285–9312, doi:10.5194/acp-15-9285-2015.

Li, X., J. Liu, and J. Yang (2006), Variation of H_2S and COS emission fluxes from *Calamagrostis angustifolia* wetlands in Sanjiang Plain, Northeast China, *Atmos. Environ.*, *40*(33), 6303–6312, doi:10.1016/j.atmosenv.2006.05.054.

Liu, J., C. Geng, Y. Mu, Y. Zhang, Z. Xu, and H. Wu (2010), Exchange of carbonyl sulfide (COS) between the atmosphere and various soils in China, *Biogeosciences*, *7*(2), 753–762, doi:10.5194/bg-7-753-2010.

Lloyd, J., and J. A. Taylor (1994), On the temperature dependence of soil respiration, *Funct. Ecol.*, *8*(3), 315–323, doi:10.2307/2389824.

Maseyk, K., L. Wingate, U. Seibt, J. Ghashghaie, C. Bathellier, P. Almeida, R. L. de Vale, J. S. Pereira, D. Yakir, and M. Mencuccini (2009), Biotic and abiotic factors affecting the $\delta^{13}C$ of soil respired CO_2 in a Mediterranean oak woodland, *Isot. Environ. Health Stud.*, *45*(4), 343–359, doi:10.1080/10256010903388212.

Maseyk, K., J. A. Berry, D. Billesbach, J. E. Campbell, M. S. Torn, M. Zahniser, and U. Seibt (2014), Sources and sinks of carbonyl sulfide in an agricultural field in the Southern Great Plains, *Proc. Natl. Acad. Sci. U.S.A.*, *111*(25), 9064–9069, doi:10.1073/pnas.1319132111.

Matthews, E. (1997), Global litter production, pools, and turnover times: Estimates from measurement data and regression models, *J. Geophys. Res.*, *102*(D15), 18,771–18,800, doi:10.1029/97JD02956.

Montzka, S., P. Calvert, B. Hall, J. Elkins, T. Conway, P. Tans, and C. Sweeney (2007), On the global distribution, seasonality, and budget of atmospheric carbonyl sulfide (COS) and some similarities to CO_2, *J. Geophys. Res.*, *112*, D09302, doi:10.1029/2006JD007665.

Navarro-García, F., M. A. Casermeiro, and J. P. Schimel (2012), When structure means conservation: Effect of aggregate structure in controlling microbial responses to rewetting events, *Soil Biol. Biochem.*, *44*, 1–8, doi:10.1016/j.soilbio.2011.09.019.

Notni, J., S. Schenk, G. Protoschill-Krebs, J. Kesselmeier, and E. Anders (2007), The missing link in COS metabolism: A model study on the reactivation of carbonic anhydrase from its hydrosulfide analogue, *ChemBioChem*, *8*(5), 530–536, doi:10.1002/cbic.200600436.

Ogawa, T., et al. (2013), Carbonyl sulfide hydrolase from *Thiobacillus thioparus* strain THI115 is one of the β-carbonic anhydrase family enzymes, *J. Am. Chem. Soc.*, *135*(10), 3818–3825, doi:10.1021/ja307735e.

Ogée, J., J. Sauze, J. Kesselmeier, B. Genty, H. Van Diest, T. Launois, and L. Wingate (2015), A new mechanistic framework to predict OCS fluxes from soils, *Biogeosci. Discuss.*, *12*(18), 15,687–15,736, doi:10.5194/bgd-12-15687-2015.

Or, D., and J. M. Wraith (2002), Soil water content and water potential relationships, in *Soil Physics Companion*, edited by M. E. Sumner, pp. 49–84, CRC Press, Boca Raton, Fla.

Placella, S. A., E. L. Brodie, and M. K. Firestone (2012), Rainfall-induced carbon dioxide pulses result from sequential resuscitation of phylogenetically clustered microbial groups, *Proc. Natl. Acad. Sci. U.S.A.*, *109*(27), 10,931–10,936, doi:10.1073/pnas.1204306109.

Protoschill-Krebs, G., and J. Kesselmeier (1992), Enzymatic pathways for the consumption of carbonyl sulphide (COS) by higher plants, *Bot. Acta*, *105*, 206–212, doi:10.1111/j.1438-8677.1992.tb00288.x.

Protoschill-Krebs, G., C. Wilhelm, and J. Kesselmeier (1996), Consumption of carbonyl sulphide (COS) by higher plant carbonic anhydrase (CA), *Atmos. Environ.*, *30*(18), 3151–3156, doi:10.1016/1352-2310(96)00026-X.

Rutledge, S., D. I. Campbell, D. Baldocchi, and L. A. Schipper (2010), Photodegradation leads to increased carbon dioxide losses from terrestrial organic matter, *Global Change Biol.*, *16*(11), 3065–3074, doi:10.1111/j.1365-2486.2009.02149.x.

Sandoval-Soto, L., M. Stanimirov, M. v. Hobe, V. Schmitt, J. Valdes, A. Wild, and J. Kesselmeier (2005), Global uptake of carbonyl sulfide (COS) by terrestrial vegetation: Estimates corrected by deposition velocities normalized to the uptake of carbon dioxide (CO_2), *Biogeosciences*, *2*(2), 125–132, doi:10.5194/bg-2-125-2005.

Schenk, S., J. Kesselmeier, and E. Anders (2004), How does the exchange of one oxygen atom with sulfur affect the catalytic cycle of carbonic anhydrase?, *Chem. Eur. J.*, *10*(12), 3091–3105, doi:10.1002/chem.200305754.

Seibt, U., L. Wingate, J. Lloyd, and J. Berry (2006), Diurnally variable $\delta^{18}O$ signatures of soil CO_2 fluxes indicate carbonic anhydrase activity in a forest soil, *J. Geophys. Res.*, *111*, G04005, doi:10.1029/2006JG000177.

Seibt, U., J. Kesselmeier, L. Sandoval-Soto, U. Kuhn, and J. Berry (2010), A kinetic analysis of leaf uptake of COS and its relation to transpiration, photosynthesis and carbon isotope fractionation, *Biogeosciences*, *7*(1), 333–341, doi:10.5194/bg-7-333-2010.

Simmons, J. S., L. Klemedtsson, H. Hultberg, and M. E. Hines (1999), Consumption of atmospheric carbonyl sulfide by coniferous boreal forest soils, *J. Geophys. Res.*, *104*(D9), 11,569–11,576, doi:10.1029/1999JD900149.

Smeulders, M. J., et al. (2011), Evolution of a new enzyme for carbon disulphide conversion by an acidothermophilic archaeon, *Nature*, *478*, 412–416, doi:10.1038/nature10464.

Stimler, K., S. A. Montzka, J. A. Berry, Y. Rudich, and D. Yakir (2010), Relationships between carbonyl sulfide (COS) and CO_2 during leaf gas exchange, *New Phytol.*, *186*(4), 869–878, doi:10.1111/j.1469-8137.2010.03218.x.

Sun, W., K. Maseyk, C. Lett, and U. Seibt (2015), A soil diffusion-reaction model for surface COS flux: COSSM v1, *Geosci. Model Dev.*, *8*, 3055–3070, doi:10.5194/gmd-8-3055-2015.

USDA Soil Survey (2014), Web Soil Survey. [Available online at http://websoilsurvey.nrcs.usda.gov/], accessed July 2014.

Van Diest, H., and J. Kesselmeier (2008), Soil atmosphere exchange of carbonyl sulfide (COS) regulated by diffusivity depending on water-filled pore space, *Biogeosciences*, *5*(2), 475–483, doi:10.5194/bg-5-475-2008.

Van Wijk, W. R., and D. A. de Vries (1963), Periodic temperature variations in a homogeneous soil, in *Physics of Plant Environment*, edited by W. R. Van Wijk, pp. 102–143, North Holland, Amsterdam, Netherlands.

Wang, J., L. Liu, X. Wang, and Y. Chen (2015), The interaction between abiotic photodegradation and microbial decomposition under ultraviolet radiation, *Global Biogeochem. Cycles*, *21*, 2095–2104, doi:10.1111/gcb.12812.

Whelan, M. E., and R. C. Rhew (2015), Carbonyl sulfide produced by abiotic thermal and photodegradation of soil organic matter from wheat field substrate, *J. Geophys. Res. Biogeosci.*, *120*, 54–62, doi:10.1002/2014JG002661.

Whelan, M. E., D.-H. Min, and R. C. Rhew (2013), Salt marsh vegetation as a carbonyl sulfide (COS) source to the atmosphere, *Atmos. Environ.*, *73*, 131–137, doi:10.1016/j.atmosenv.2013.02.048.

Whelan, M. E., T. W. Hilton, J. Berry, M. Berkelhammer, A. R. Desai, and J. E. Campbell (2015), Carbonyl sulfide exchange in soils for better estimates of ecosystem carbon uptake, *Atmos. Chem. Phys. Discuss.*, *15*, 21,095–21,132, doi:10.5194/acpd-15-21095-2015.

Wingate, L., U. Seibt, K. Maseyk, J. Ogée, P. Almeida, D. Yakir, J. S. Pereira, and M. Mencuccini (2008), Evaporation and carbonic anhydrase activity recorded in oxygen isotope signatures of net CO_2 fluxes from a Mediterranean soil, *Global Change Biol.*, *14*(9), 2178–2193, doi:10.1111/j.1365-2486.2008.01635.x.

Wingate, L., et al. (2009), The impact of soil microorganisms on the global budget of $\delta^{18}O$ in atmospheric CO_2, *Proc. Natl. Acad. Sci. U.S.A.*, *106*(52), 22,411–22,415, doi:10.1073/pnas.0905210106.

Yi, Z., X. Wang, G. Sheng, D. Zhang, G. Zhou, and J. Fu (2007), Soil uptake of carbonyl sulfide in subtropical forests with different successional stages in south China, *J. Geophys. Res.*, *112*, D08302, doi:10.1029/2006JD008048.

Yi, Z., X. Wang, G. Sheng, and J. Fu (2008), Exchange of carbonyl sulfide (OCS) and dimethyl sulfide (DMS) between rice paddy fields and the atmosphere in subtropical China, *Agric. Ecosyst. Environ.*, *123*, 116–124, doi:10.1016/j.agee.2007.05.011.

Yi, Z., L. Zheng, T. Wu, and X. Wang (2013), Contribution of aboveground plants, the rhizosphere and root-free-soils to total COS and DMS fluxes at three key growth stages in rice paddies, *Agric. Ecosyst. Environ.*, *179*, 11–17, doi:10.1016/j.agee.2013.07.005.